



## Unveiling microbial electricity driven anoxic ammonium removal

Miguel Osset-Álvarez<sup>a</sup>, Narcis Pous<sup>a</sup>, Paola Chiluiza-Ramos<sup>b</sup>, Lluís Bañeras<sup>b</sup>, M. Dolors Balaguer<sup>a</sup>, Sebastià Puig<sup>a,\*</sup>

<sup>a</sup> LEQUIA, Institute of Environment, University of Girona, Campus Montilivi, Maria Aurèlia Capmany 69, E-17003 Girona, Catalonia, Spain

<sup>b</sup> Molecular Microbial Ecology Group (gEMM-IEA), Institute of Aquatic Ecology, Faculty of Sciences, University of Girona, Campus Montilivi, Maria Aurèlia Capmany 40, E-17003 Girona, Catalonia, Spain

### ARTICLE INFO

#### Keywords:

Bioelectrochemical systems  
Microbial anode  
Nitrogen removal  
Wastewater treatment

### ABSTRACT

Microbial electricity-driven anoxic ammonium removal could remove ammonium from wastewater without the presence of oxygen (aeration) using electricity. This study aims at unveiling the potential biologic pathways for the bioelectrochemical oxidation of ammonium to dinitrogen gas in an anaerobic bioelectrochemical system (BES). Known intermediate metabolites of this process (hydroxylamine, nitrite and nitrate) were monitored in two BES replicates. Ammonium was fully oxidized to dinitrogen gas without intermediates accumulation in the anodic chamber. *Achromobacter* sp. was the most abundant microorganism (up to 60%, according to sequence reads) in the mixed community. Hydroxylamine and nitrite oxidation were electroactive processes, reinforcing the role of the anodic electrode as the electron acceptor for ammonium oxidation. Taking it all together, ammonium can be removed in BES by a combination of different bio/electrochemical processes. A deeper understanding on how the different metabolisms are coupled together is required for increasing the current ammonium removal rates.

### 1. Introduction

Bioelectrochemical systems (BES) are an innovative approach to accelerate bioremediation processes by supplying an unlimited source of electron donors/acceptors to bacteria. Biologic nitrogen removal is one of the bioremediation processes that could take profit of BES. The external supply of oxygen (oxygen (O<sub>2</sub>), electron acceptor) and organic matter (electron donor) is usually required to carry out nitrification/denitrification reactions. The usage of an anodic electrode as an electron acceptor for microbial ammonium (NH<sub>4</sub><sup>+</sup>) oxidation could reduce the need of aeration and the important associated costs (Vilajeliu-Pons et al., 2018).

Recently, Shaw et al. (2020) demonstrated a new mechanism for ammonium bioelectrochemical oxidation to dinitrogen gas (N<sub>2</sub>) in a BES inoculated with ANAMMOX culture and a polarized anode electrode at different potentials from −0.1 to +0.6 V vs. SHE. The ammonium oxidation mechanism started with the oxidation of NH<sub>4</sub><sup>+</sup> to NH<sub>2</sub>OH, which reacted with an additional molecule of NH<sub>4</sub><sup>+</sup> to form hydrazine (N<sub>2</sub>H<sub>4</sub>), an ANAMMOX-specific intermediary metabolite (Van Teeseling et al., 2013), and it ended up with the oxidation of N<sub>2</sub>H<sub>4</sub> to N<sub>2</sub>. This process hereafter referred as electro-ANAMMOX, where neither nitrite

(NO<sub>2</sub><sup>−</sup>) nor nitrate (NO<sub>3</sub><sup>−</sup>) were generated or consumed, has been only reported for ANAMMOX bacteria. ANAMMOX-like bacteria such as Feammox have been reported to present electroactive activity (Ruiz-Urigüen et al., 2019; Zhu et al., 2021). Ruiz-Urigüen et al. (2019) suggested that Feammox (*Acidimicrobiaceae* sp. A6) oxidized NH<sub>4</sub><sup>+</sup> to nitrite, which was later reduced to N<sub>2</sub> due to the presence of iron (Fe<sup>2+</sup>) in the medium. Such a behaviour (NH<sub>4</sub><sup>+</sup> oxidation to NO<sub>2</sub><sup>−</sup>/NO<sub>3</sub><sup>−</sup>) is the one that would be expected for nitrifying bacteria. Indeed, in some works, the usage of nitrifying bacteria in presence of a polarized electrode have reported the conversion of NH<sub>4</sub><sup>+</sup> into NO<sub>2</sub><sup>−</sup>/NO<sub>3</sub><sup>−</sup>, which can be later converted into N<sub>2</sub> by promoting processes such as ANAMMOX or heterotrophic denitrification (Koffi and Okabe, 2021; Qu et al., 2014; Tutar Oksuz and Beyenal, 2021; Zhou et al., 2021; Zhu et al., 2016).

However, in other works where no organic matter was present and the anodic microbial community presented a high abundance of nitrifiers, almost undetectable amounts of ANAMMOX, the ammonium conversion into dinitrogen gas (N<sub>2</sub>) has been observed (Siegert and Tan, 2019; Vilajeliu-Pons et al., 2018; Zhan et al., 2014). Different interpretations have been elucidated. For example, Zhan and co-workers (2014), who used an inoculum from a wastewater treatment plant (WWTP) and set an anodic potential of +0.6 V vs Ag/AgCl, attributed

\* Corresponding author.

E-mail address: [sebastia.puig@udg.edu](mailto:sebastia.puig@udg.edu) (S. Puig).

<https://doi.org/10.1016/j.biteb.2022.100975>

Received 31 January 2022; Received in revised form 1 February 2022; Accepted 1 February 2022

Available online 5 February 2022

2589-014X/© 2022 The Authors.

Published by Elsevier Ltd.

This is an open access article under the CC BY-NC-ND license

(<http://creativecommons.org/licenses/by-nc-nd/4.0/>).

the absence of  $\text{NO}_2^-$  and  $\text{NO}_3^-$  accumulation to the presence of denitrifying bacteria in the anodic biofilm (*Comamonas* sp. and *Paracoccus* sp.), even though no organic matter was supplemented to the medium (Zhan et al., 2014). Siegert and Tan (2019), who tested different anodic potentials from +0.15 to +0.55 V vs. SHE, observed a similar behaviour and they considered that denitrification could have a role in the cathode compartment. In Vilajeliu-Pons et al. (2018), the anode of a BES reactor was inoculated with different nitrifying bacteria and poised at +0.8 V vs. SHE. From the results obtained, it was estimated that *Nitrosomonas* was the main responsible for the bioelectrochemical oxidation of  $\text{NH}_4^+$  and hydroxylamine ( $\text{NH}_2\text{OH}$  – nitrification intermediate), while very low concentrations of  $\text{NO}_2^-$  and  $\text{NO}_3^-$  were detected due to a combination of ANAMMOX and denitrification processes.

Without a better understanding of the underlying processes, an optimization of the operational conditions and the reactor setup might be threatened. For this reason, this work aimed at elucidating how  $\text{NH}_4^+$  could be bioelectrochemically oxidized with a low presence (or absence) of ANAMMOX bacteria. A series of experiments were set up in two parallel fed-batch BES to study the removal of ammonium and other nitrogen species (nitrate, nitrite and hydroxylamine) that could be possibly involved in the process.

## 2. Materials and methods

### 2.1. Experimental set-up

Two BES were constructed using two rectangular methacrylate structures containing two 1 L chambers (anode and cathode) separated by an anion exchange membrane (AMI-7001, Membranes International Inc., USA) (Vilajeliu-Pons et al., 2018). The anion exchange membrane was used to minimize the diffusion of ammonium to the cathodic compartment (Kim et al., 2008). Each chamber was filled with granular graphite (model 00541, 1.5–5 mm diameter, EnViro-cell, Germany). Laboratory tests indicated that the bed of granular graphite presented a specific electric resistivity of  $1.2 \cdot 10^{-3} \pm 0.1 \cdot 10^{-4}$  Ohm·m. Elemental composition is shown in Table S1. An Ag/AgCl reference electrode was inserted in the anode compartment (+0.197 V vs. SHE, model RE-5B, BASI, UK), and two graphite rods (3 mm radius x 130 mm length, Sofacel, Spain) were placed as current collectors in each chamber. The net liquid volume of each chamber was 0.4 L. A potentiostat (Model VSP, BioLogic, France) connected the anode/cathode current collectors and the reference electrode to polarize the working electrode (anode) at +0.8 V vs. SHE.

Each chamber was connected to a 2 L tank using a peristaltic pump (model 205S, Watson Marlow, UK), with a recirculation flow of 7.5 L day<sup>-1</sup> and later increased to 25 L day<sup>-1</sup> (model 323 E/D, Watson Marlow, UK) to ensure a better flow distribution inside the reactor.

### 2.2. Inoculation and experimental procedure

The anodic compartments and buffers tanks of the BES were inoculated with a solution containing 50% (V/V) of an inoculum that consisted of a 1:1 mix of biomass obtained from a partial nitrification reactor (Gabarró et al., 2012) and an aerobic nitrification reactor of an urban WWTP (Girona, Spain). Solution media contained 0.195 g  $\text{NH}_4\text{Cl}$  L<sup>-1</sup> (corresponding to 50 mg N- $\text{NH}_4^+$  L<sup>-1</sup>), 1.05 g  $\text{NaHCO}_3$  L<sup>-1</sup>, 0.015 g  $\text{CaCl}_2$  L<sup>-1</sup>, 0.1 g  $\text{MgSO}_4 \cdot 7 \text{H}_2\text{O}$  L<sup>-1</sup>, 0.162 g  $\text{Na}_2\text{HPO}_4$  L<sup>-1</sup>, 0.25 g  $\text{NaCl}$  L<sup>-1</sup>, 1.072 g  $\text{KH}_2\text{PO}_4$  L<sup>-1</sup> and 0.1 mL L<sup>-1</sup> of trace elements solution (Rabaey et al., 2005). The same solution, but without inoculum, was used in the cathode.

The system was operated in batch mode during both inoculation and operation, with 6 mL samples being taken twice a week from both compartments (anode and cathodes) of the reactors. The volume sampled was immediately replaced with fresh medium. Each 2 L tank was flushed with  $\text{N}_2$  for 15 min before each batch experiment to avoid air intrusion and hence ensure anoxic conditions. 1 L gas-tight bags

(Standard FlexFoil® Sample bag, SCK, UK) were filled with  $\text{N}_2$  and connected to the tanks, with the gas being regularly replaced. During the inoculation phase, once  $\text{NH}_4^+$  was exhausted for the first time, the medium in the anode was replaced with fresh inoculum solution (containing 50 mg N- $\text{NH}_4^+$  L<sup>-1</sup>), while a new abiotic ammonium-rich solution replaced the medium present in the cathode. When consistent  $\text{NH}_4^+$  removal was observed at the anode (30 days after starting the experiment), the solution in the cathode was changed to a solution without ammonium, and the inoculation phase was finished.

During the operational period, before anodic  $\text{NH}_4^+$  was depleted, the anode was spiked with an  $\text{NH}_4^+:\text{HCO}_3^-$  solution (1:2 M ratio) to increase the anodic ammonium concentration to 50 mg N- $\text{NH}_4^+$  L<sup>-1</sup> to study ammonium removal in the long-term. Different experiments were performed to study the effect of transient accumulation of intermediate metabolites (nitrate, nitrite and hydroxylamine) on ammonium removal. After 180 days of operation, known amounts of intermediates were added in the anode or the cathode compartments in separate experiments (Table 1). Moreover, control tests were performed in the buffer tanks of the anode and the cathode to check whether ammonium was removed or not inside those tanks. Buffer tanks were disconnected from the BES and 5-days control tests were carried out by adding fresh intermediary metabolites (nitrite, nitrate) and ammonium in the buffer tanks. Finally, abiotic electrochemical tests with granular graphite were also conducted to elucidate the possible catalyzing role of granular graphite (see SI3 for full description).

### 2.3. Analyses and calculations

The concentrations of  $\text{NH}_4^+$ ,  $\text{NO}_2^-$  and  $\text{NO}_3^-$  were measured by ion chromatography (Dionex IC5000, Vertex Technics, Spain). pH was determined with a pH-meter (pH-meter basic 20+, Crison, Spain). The concentration of hydrazine ( $\text{N}_2\text{H}_4$ ) was measured using a colourimetric kit (Spectroquant® Hydrazine test 109,711, Merck, Germany) The concentration of hydroxylamine ( $\text{NH}_2\text{OH}$ ) was determined colourimetrically (Oshiki et al., 2016). Nitrous oxide ( $\text{N}_2\text{O}$ ) was occasionally monitored in the recirculation loop of each compartment using an  $\text{N}_2\text{O}$  liquid-phase microsensors (Unisense, Denmark). Oxygen probes (model 6050, detection limit 0.1 mg  $\text{O}_2$  L<sup>-1</sup>, Mettler Toledo, USA) were permanently installed in the anodic compartment to have a continuous measurement of the concentration of dissolved oxygen in the medium.

Linear regression of the first data points (i.e. initial activities) was used to estimate the removal rates of nitrogen species in the experiments involving nitrate or nitrite.

Electron balances for the different potential electron donors/acceptors using the anode/cathode as electron sink/supply were performed through the calculation of the Coulombic efficiency for the different possible reactions (CE, %) (Eq. (1)).

$$\text{CE} (\%) = 100\% \times C_{\text{measured}} / C_{\text{theoretic}} \quad (1)$$

Where  $C_{\text{measured}}$  means the coulombs measured in the potentiostat (C) and  $C_{\text{theoretic}}$  means the coulombs theoretically generated/required from the oxidation/reduction of an electron donor/acceptor as described in Eq. (2).

$$C_{\text{theoretic}} = \frac{-\Delta a \times n \times F}{14 \text{ g N/mol N}} \quad (2)$$

Where  $F$  is the Faraday constant (96,485C/mol of electrons),  $a$  equals to the mass of the nitrogen specie substrate targeted in the different tests (g N) (i.e. N- $\text{NH}_4^+$ , N- $\text{NH}_2\text{OH}$ , N- $\text{NO}_2^-$ , and N- $\text{NO}_3^-$ ), and  $n$  is the mols of electrons required to oxidize/reduce 1 mol N of the different nitrogen species targeted in the different tests (mol of electrons/ mol N). The possible reactions considered in the different tests and theirs corresponding  $n$  values were: a)  $\text{NH}_4^+$  oxidation to  $\text{N}_2$  ( $n = 3$ );  $\text{NH}_2\text{OH}$  oxidation to  $\text{NO}$  ( $n = 3$ );  $\text{NH}_2\text{OH}$  oxidation to  $\text{N}_2$  ( $n = 1$ );  $\text{NO}_2^-$  oxidation to  $\text{NO}_3^-$  ( $n = 2$ );  $\text{NO}_3^-$  reduction to  $\text{N}_2$  ( $n = 5$ ). Following the following

**Table 1**  
Nitrogen species fed to the BES at the different experiments performed.

Experiment (no. of batches)	Nitrogen species added		Time	Initial concentration (mg N L <sup>-1</sup> )					
	Anode	Cathode		NH <sub>4</sub> <sup>+</sup> anode	NO <sub>3</sub> <sup>-</sup> cathode	NO <sub>3</sub> <sup>-</sup> anode	NO <sub>2</sub> <sup>-</sup> cathode	NO <sub>2</sub> <sup>-</sup> anode	NH <sub>2</sub> OH anode
Exp. 1 (8)	NH <sub>4</sub> <sup>+</sup>	–	265 d	14–52					
Exp. 2A (2)	NH <sub>4</sub> <sup>+</sup>	NO <sub>2</sub> <sup>-</sup>	9 d	42–41			61–75		
Exp. 2B (4)	NH <sub>4</sub> <sup>+</sup> + NO <sub>2</sub> <sup>-</sup>	–	15 d	27–86				54–139	
Exp. 2C (2)	NO <sub>2</sub> <sup>-</sup>	–	14 d					40–46	
Exp. 3 (4)	NH <sub>4</sub> <sup>+</sup> + NH <sub>2</sub> OH	–	6 h	22–32					15
Exp. 4A (2)	NH <sub>4</sub> <sup>+</sup>	NO <sub>3</sub> <sup>-</sup>	12 d	29–39	39–42				
Exp. 4B (2)	NH <sub>4</sub> <sup>+</sup> + NO <sub>3</sub> <sup>-</sup>	–	14 d	49–73			35–40		
Exp. 4C (2)	NO <sub>3</sub> <sup>-</sup>	–	33 d				46–68		

CEs were calculated in the different conditions tested: a) CE (NH<sub>4</sub><sup>+</sup>/N<sub>2</sub>) were calculated for Experiments 1; b) CE (NO<sub>2</sub><sup>-</sup>/NO<sub>3</sub><sup>-</sup>) were calculated for Experiments 2; c) CE (NH<sub>2</sub>OH/NO) and CE (NH<sub>2</sub>OH/N<sub>2</sub>) were calculated for Experiments 3 and d) CE (NO<sub>3</sub><sup>-</sup>/N<sub>2</sub>) were calculated for Experiments 4.

The area of the electrode ( $A_{\text{electrode}}$ , m<sup>2</sup>) to estimate the current density in the reactor (mA m<sup>-2</sup>) was calculated according to Eq. (3)

$$A_{\text{electrode}} = A_{\text{GG}} \times V_{\text{TotalGG}} / V_{\text{GG}} \quad (3)$$

Where  $A_{\text{GG}}$  means the area of a graphite granule (m<sup>2</sup>), considering each granule as a perfect sphere of 0.004 m diameter (mean diameter according to manufacturer specifications as shown above),  $V_{\text{TotalGG}}$  means the total volume of granular graphite in the anodic compartment (0.0006 m<sup>3</sup>) and  $V_{\text{GG}}$  means the volume of one single graphite granule (m<sup>3</sup>).

#### 2.4. Microbial analyses

DNA was extracted from graphite granules as described previously (Vilajeliu-Pons et al., 2016). Briefly, granules were incubated in a water ultrasonic bath for 60 s, detached biofilm and cells were collected by centrifugation and cells pellets were used for extraction of nucleic acids cells using the Fast DNA SPIN Kit for Soil (MP Biomedicals, USA) following the recommended instructions. Partial sequences of the bacterial and archaeal 16S rRNA genes were obtained using the Illumina MiSeq PE250 sequencing platform with primers 515F-806R targeting the V4 region (Kozich et al., 2013). Sequencing was conducted by the RTSF Core facilities (Michigan State University, USA, <https://rtsf.atsci.msu.edu/>).

Sequence quality filtering, trimming, dereplicating, and merging were performed using the DADA2 based pipeline implemented in R as recommended (Callahan et al., 2016). Basic filtering methods were set to 230 bp and 180 bp for forward and reverse reads, no ambiguous bases allowed, and maximum expected error rates of 2. Singletons were removed from the final set of sequences to avoid spurious diversity. Sequences were clustered into amplicon sequence variants (ASV, 100% similarity index). Bimeras were detected and removed (172 out of 1395 ASV) using the consensus method implemented in DADA2 package. Finally, taxonomic assignments were performed at the maximum taxonomic rank when possible, using the Silva v132 train set to release as a reference. Relative abundances of selected taxons and microbiome graphical representations were performed using the Phyloseq package (McMurdie and Holmes, 2012) implemented in R. Whenever it was necessary due to poor taxonomical assignment with the used reference dataset, ASVs were assigned taxonomically using nucleotide Blast searches at NCBI.

### 3. Results and discussion

#### 3.1. Performance of the BES under an ammonium-rich medium

Duplicate BES reactors were operated in batch mode for 550 days

(Fig. S2 and S3). A representative batch profile of ammonium removal was selected as a control test (Experiment 1) and depicted in Fig. 1. Ammonium was removed at a constant rate (4.8 g N-NH<sub>4</sub><sup>+</sup> m<sup>-3</sup> d<sup>-1</sup> in the anode, Table 2), while the current density remained stable (0.44 mA m<sup>-2</sup>). This rate was found to be lower than previous studies where bioelectrochemical anoxic ammonium removal was tested without the presence of organic matter (Siegert and Tan, 2019; Vilajeliu-Pons et al., 2018; Zhan et al., 2014). For example, Vilajeliu-Pons et al. (2018) observed an ammonium removal rate of 35 ± 10 gN·m<sup>-3</sup>·d<sup>-1</sup> when operating the system under the continuous-flow mode, while Zhan et al. (2014) observed a removal of 60 gN·m<sup>-3</sup>·d<sup>-1</sup> in batch experiments. Considering the possible biologic ammonium removal processes (i.e. nitrification, denitrification), no nitrite, nitrous oxide nor nitrate accumulation were observed. Ammonium removal via free ammonia (NH<sub>3</sub>) volatilization was not likely to occur to a high extent at the working pH (7.6). Under these conditions, NH<sub>3</sub> represented a maximum of 2% of the ammonium present in the system (NH<sub>3</sub>/NH<sub>4</sub><sup>+</sup> pK<sub>a</sub> of 9.25). Moreover, the reactors were tightly closed during all the experimental periods to avoid any gas leakage. The small amounts of NH<sub>3</sub> possibly present in the system could diffuse from the anode to the cathode chamber, giving a reasonable explanation to the slight changes in the cathodic NH<sub>4</sub><sup>+</sup> concentration observed (Fig. 1).

Conventional nitrification uses oxygen as an electron acceptor. However, ammonium oxidation in the reactors most likely occurred under anoxic conditions. The concentration of dissolved oxygen remained below the oxygen probe detection limit of 0.1 mg O<sub>2</sub> L<sup>-1</sup>, and abiotic batch tests previously performed in identical reactors and under the same anodic potential demonstrated that oxygen was not electrochemically produced in the system (Vilajeliu-Pons et al., 2018). On the top of that, Lai and co-workers (2017) observed that graphite electrodes (the ones used in the current work) poised at high anodic potentials (+1.2 V vs. SHE) did graphite oxidation to CO<sub>2</sub> instead of H<sub>2</sub>O oxidation to O<sub>2</sub> (Lai et al., 2017). Abiotic tests performed by Vilajeliu-Pons et al. (2018) also showed no ammonium removal, indicating that NH<sub>4</sub><sup>+</sup> oxidation in BES was a bioelectrochemical rather than a pure electrochemical process. Moreover, Vilajeliu-Pons et al. (2018) proved that the addition of allylthiourea (ATU), a selective inhibitor of ammonium oxidation to nitrite, ceased both electric current and ammonium removal, confirming the role of these microorganisms in electricity-driven NH<sub>4</sub><sup>+</sup> oxidation. In the experimental set-up used (Fig. S1), one might hypothesize that ammonium could be removed either in the BES reactor or in the buffer tanks used to support the recirculation loop. In addition to these previous tests, control tests were performed in the buffer tanks alone to elucidate the influence of the BES on ammonium removal. Negligible removals of ammonium or nitrate were observed, indicating that these reactions were only taking place in the BES. Thus, the tests performed assumed that ammonium was removed via an electricity-driven process in the absence of oxygen. Assuming an oxidation of NH<sub>4</sub><sup>+</sup> to N<sub>2</sub>, an average coulombic efficiency of 108% could be estimated (Experiment 1, Table 2). This suggested that the current flow detected in the system corresponded to approximately 3 electrons per mole of NH<sub>4</sub><sup>+</sup> oxidized. Different tests with possible nitrogen species intermediates were performed to elucidate these possible reactions.

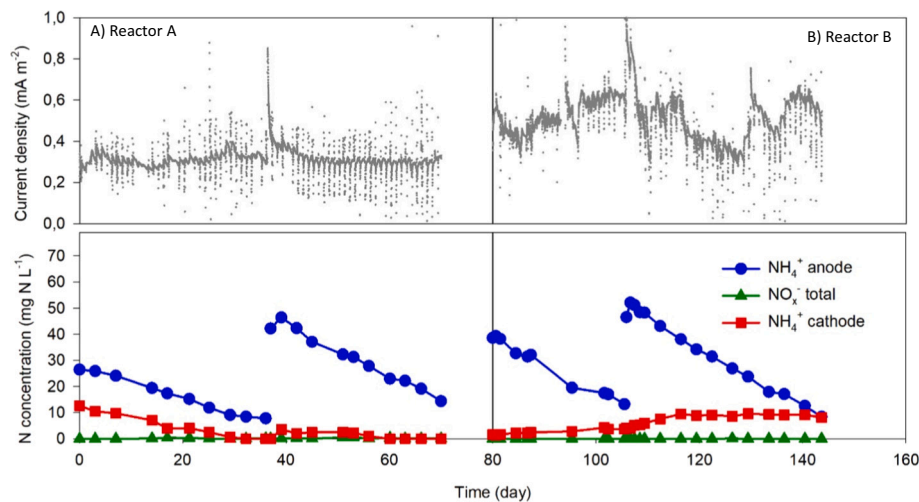


**Fig. 1.** Representative batch tests for Experiment 1. Time evolution of nitrogen species content ( $\text{NO}_x^-$  total refers to  $\text{NO}_2^- + \text{NO}_3^-$ ) and current density after adding  $\text{NH}_4^+$  at the anode of reactors A (A, left) and B (B, right).

**Table 2**

Removal rates of nitrogen species concentration and coulombic efficiencies in the different experiments performed in this study.

Experiment (no. of batches)	Experiment 1 (8)	Experiment 2A (2)	Experiment 2B (4) <sup>a</sup>	Experiment 2C (2)	Experiment 4A (2)	Experiment 4B (2)	Experiment 4C (2)
Species involved	$\text{NH}_4^+$	$\text{NO}_2^- + \text{NH}_4^+$		$\text{NO}_2^-$	$\text{NO}_3^- + \text{NH}_4^+$		$\text{NO}_3^-$
Time (days) <sup>b</sup>	264.8	3.2	11.4	3.3	3.4	3.3	9.5
$\Delta\text{NH}_4^+$ an. ( $\text{g N m}^{-3}\text{d}^{-1}$ )	$-4.8 \pm 2.5$	$-18.0 \pm 1.3$	$-17.9 \pm 5.9$	$0.0 \pm 0.0$	$-3.5 \pm 5.7$	$-11.9 \pm 1.9$	$0.2 \pm 0.4$
$\Delta\text{NO}_2^-$ an. ( $\text{g N m}^{-3}\text{d}^{-1}$ )	$0.0 \pm 0.0$	$35.4 \pm 11.7$	$-81.7 \pm 25.7$	$-48.7 \pm 6.5$	$1.5 \pm 1.1$	$-0.5 \pm 0.7$	$0.7 \pm 0.3$
$\Delta\text{NO}_3^-$ an. ( $\text{g N m}^{-3}\text{d}^{-1}$ )	$0.0 \pm 0.0$	$5.7 \pm 5.4$	$3.5 \pm 3.9$	$9.5 \pm 10.1$	$27.5 \pm 12.2$	$-74.6 \pm 2.5$	$-29.5 \pm 4.4$
$\Delta\text{NH}_4^+$ ca. ( $\text{g N m}^{-3}\text{d}^{-1}$ )	$-0.3 \pm 1.0$	$4.8 \pm 2.9$	$9.4 \pm 11.4$	$6.8 \pm 2.4$	$2.1 \pm 3.0$	$3.5 \pm 4.1$	$0.3 \pm 1.2$
$\Delta\text{NO}_2^-$ ca. ( $\text{g N m}^{-3}\text{d}^{-1}$ )	$0.0 \pm 0.0$	$-87.4 \pm 35.7$	$4.1 \pm 6.3$	$17.7 \pm 8.5$	$4.2 \pm 1.0$	$1.3 \pm 0.3$	$1.7 \pm 1.8$
$\Delta\text{NO}_3^-$ ca. ( $\text{g N m}^{-3}\text{d}^{-1}$ )	$0.0 \pm 0.0$	$2.7 \pm 2.3$	$2.0 \pm 0.8$	$2.1 \pm 0.5$	$-83.0 \pm 5.7$	$16.1 \pm 0.8$	$4.0 \pm 5.8$
Coulombic efficiency	Reaction	$\text{NH}_4^+ \rightarrow \text{N}_2$	$\text{NO}_2^- \rightarrow \text{NO}_3^-$		$\text{NO}_3^- \rightarrow \text{N}_2$		
	(%)	$108 \pm 83$	$63 \pm 20$	$65 \pm 23$	$175 \pm 5$	$2 \pm 0$	$2 \pm 0$

<sup>a</sup> The first batch from Fig. 2B was not used for the calculations of removal rates because ammonium was depleted before nitrite.

<sup>b</sup> Time refers to the period used to determine the removal rates in each experiment, not to the complete duration of the experiments. The data from Experiment 3 were not included in this table because that experiment took place in very short time (6 h) and only the concentration of hydroxylamine changed during that experiment.

Results obtained are presented in the following sections.

### 3.2. Performance of the BES under a nitrite-rich medium

In conventional nitrification processes, nitrite is the main intermediary metabolite. Its role on the overall BES process was investigated by performing different tests (Table 1, Fig. 2), including: A) addition of nitrite to the cathode with ammonium present at the anode (Experiment 2A); B) addition of nitrite to the anode while  $\text{NH}_4^+$  was present at the anode (Experiment 2B); and C) addition of  $\text{NO}_2^-$  at the anode with no ammonium present at the reactor (Experiment 2C).

Nitrite was rapidly consumed in all tests. Focusing, first, on ammonium removal in Experiments 2,  $\text{NH}_4^+$  removal rate was faster in the experiments where nitrite was present (Experiment 2A,  $18.0 \text{ g N-NH}_4^+ \text{ m}^{-3} \text{ d}^{-1}$  and Experiment 2B,  $17.9 \text{ g N-NH}_4^+ \text{ m}^{-3} \text{ d}^{-1}$ ) than when  $\text{NH}_4^+$  was alone (Experiment 1,  $4.8 \text{ g N-NH}_4^+ \text{ m}^{-3} \text{ d}^{-1}$ ). It suggested that, somehow, ammonium promoted nitrite reduction, which could imply some ANAMMOX-like activity in the reactor (Kartal et al., 2011). However, the nitrite removal rates ( $41.7\text{--}87.4 \text{ g N-NO}_2^- \text{ m}^{-3} \text{ d}^{-1}$ ) were much higher than the observed ammonium removal rates. This indicated that any nitrite generated from ammonium oxidation was rapidly removed from the reactor, avoiding any detectable nitrite accumulation. Interestingly, nitrite removal was faster in the tests where ammonium was present in the medium (Experiment 2A,  $87.4 \text{ g N-NO}_2^- \text{ m}^{-3} \text{ d}^{-1}$  at

the cathode and Experiment 2B,  $81.7 \text{ g N-NO}_2^- \text{ m}^{-3} \text{ d}^{-1}$  at the anode) than in the tests where nitrite was spiked alone (Experiment 2C ( $41.7 \text{ g N-NO}_2^- \text{ m}^{-3} \text{ d}^{-1}$  at the anode) (Fig. 2, Table 2). The increase on ammonium removal rate in presence of nitrite ( $13.2\text{--}13.1 \text{ g N-NH}_4^+ \text{ m}^{-3} \text{ d}^{-1}$ ) would require an increase of nitrite removal rate of  $17.4\text{--}17.2 \text{ g N-NO}_2^- \text{ m}^{-3} \text{ d}^{-1}$  if the ANAMMOX process is considered ( $\text{NH}_4^+:\text{NO}_2^-$  1:1.32). While the increase observed on nitrite removal rate in presence of ammonium was  $45.7\text{--}40 \text{ g N-NO}_2^- \text{ m}^{-3} \text{ d}^{-1}$ . Therefore, an ANAMMOX-like process cannot fully explain the whole of the differences observed on nitrite removal rate in the presence/absence of ammonium. Putative ANAMMOX activity could be further elucidated by analyzing the concentration of hydrazine ( $\text{N}_2\text{H}_4$ ), a metabolite only generated during ANAMMOX reaction (Van Teeseling et al., 2013). Hydrazine was measured 24 h after the start of Experiments 2A and 2B, as well as when nitrite was completely consumed in Experiment 2A (Fig. 2). The concentration of  $\text{N}_2\text{H}_4$  was  $0.5 \text{ mg N-N}_2\text{H}_4 \text{ L}^{-1}$  at the anode and  $1.7 \text{ mg N-N}_2\text{H}_4 \text{ L}^{-1}$  at the cathode for Experiment 2A and  $1.1 \text{ mg N-N}_2\text{H}_4 \text{ L}^{-1}$  at the anode and  $0.3 \text{ mg N-N}_2\text{H}_4 \text{ L}^{-1}$  at the cathode for Experiment 2B. When nitrite was fully depleted, hydrazine content was negligible (less than  $0.01 \text{ mg N-N}_2\text{H}_4 \text{ L}^{-1}$  at each chamber at the end of Experiment 2A). Collectively, differences in the hydrazine concentrations confirmed that ANAMMOX-like processes could be taking place in the BES.

It is worth noting that current density increased steeply (reaching a



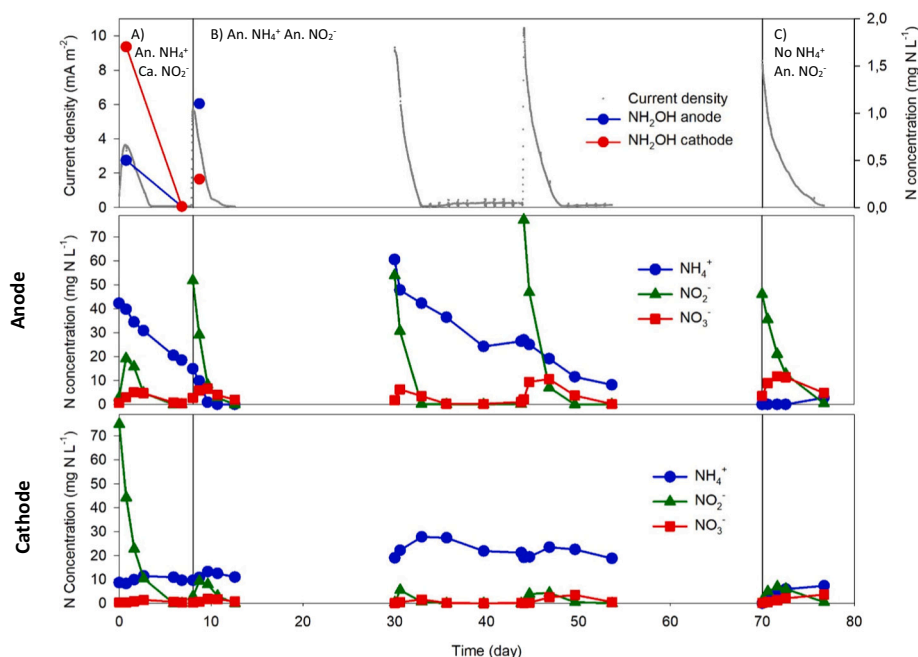


**Fig. 2.** Representatives batch tests for Experiment 2 in Reactor A. Evolution of nitrogen species concentration and current density (top), nitrogen species concentration at the anode (middle) and nitrogen species at the cathode (bottom). A) Experiment 2A: addition of  $\text{NO}_2^-$  to the cathode with  $\text{NH}_4^+$  present at the anode (left). B) Experiment 2B: addition of  $\text{NO}_2^-$  to the anode with  $\text{NH}_4^+$  present at the anode (centre). C) Experiment 2C: addition of  $\text{NO}_2^-$  to the anode with no  $\text{NH}_4^+$  present at the anode (right).

maximum value of  $10.5 \text{ mA m}^{-2}$ ) after nitrite addition and it subsequently plummeted to basal values together with the consumption of  $\text{NO}_2^-$  (Fig. 2). In Experiments 2B and 2C, this current density trend appeared right after nitrite was added to the anode. However, it was not observed immediately after spiking  $\text{NO}_2^-$  to the cathode (Experiment 2A). Instead, the current density increased progressively, and it coincided with the migration of nitrite to the anode (Fig. 2). The maximum current and anodic  $\text{NO}_2^-$  concentration were reached at the same time, being both smaller than those observed when nitrite was directly added at the anode. This indicated that the current rise was generated by an anodic-specific process involving  $\text{NO}_2^-$ . One might hypothesize that the increase of current density could be attributed to a bioelectrochemical  $\text{NO}_2^-$  oxidation with the anode electrode serving as an electron acceptor. From the author's best knowledge, it would be the first time that bioelectrochemical nitrite oxidation to nitrate using an anode as an electron acceptor would be suggested. Transient anodic  $\text{NO}_3^-$  accumulation was observed in all three nitrite experiments, and then nitrate was removed ( $5.7 \text{ g N-NO}_3^- \text{ m}^{-3} \text{ d}^{-1}$  for Experiment 2A,  $3.5 \text{ g N-NO}_3^- \text{ m}^{-3} \text{ d}^{-1}$  for Experiment 2B and  $9.5 \text{ g N-NO}_3^- \text{ m}^{-3} \text{ d}^{-1}$  for Experiment 2C). Abiotic tests performed with nitrite and granular graphite as electrode also showed an increase of current density linked to nitrite removal (Fig. S4), but in this case, all the  $\text{NO}_2^-$  removed was accumulated in the form of  $\text{NO}_3^-$ , without further processing. No abiotic nitrite oxidation had been observed previously when using graphite rods (Vilajeliu-Pons et al., 2018). Thus, the reason behind abiotic oxidation can be found in the higher level of impurities present on granular graphite compared to graphite rods (Table S11). Results observed in abiotic tests indicated that the oxidation of nitrite to nitrate in a BES was an anodic electrochemical and/or bioelectrochemical process. However, no  $\text{NO}_3^-$  accumulation was detected in BES reactors, instead a full conversion to  $\text{N}_2$  was observed. Since it cannot be expected that pure electrochemical  $\text{NO}_2^-$  oxidation to  $\text{NO}_3^-$  was avoided in the BES, it must be hypothesized that a microbial-mediated process was in charge of the later conversion of  $\text{NO}_3^-$  to  $\text{N}_2$ . How this process occurred remains unknown (Fig. 2).

Under the hypothesis that all the nitrite removed from the system was previously oxidized to nitrate, the coulombic efficiency of the oxidation of  $\text{NO}_2^-$  to  $\text{NO}_3^-$  in Experiment 2C (nitrite alone) was 175%. Thus, nitrite oxidation to nitrate alone could not explain the whole increase of current observed, but the spike of nitrite could have initiated a

cyclic process where nitrite was electrochemical/bioelectrochemically converted to nitrate, which, at the same time, was reduced into nitrite, explaining the over-current observed. However, the observation of nitrite and nitrate decreasing along the process indicated the existence of other parallel reactions involving nitrite, so the cyclic process would come to an end when all the  $\text{NO}_2^-$  and  $\text{NO}_3^-$  were removed (reduced to  $\text{N}_2$ ). This could explain why the coulombic efficiency of the  $\text{NO}_2^-$  oxidation was lower in the experiments involving ammonium and nitrite, 2A and 2B (63% and 65% respectively), which accounted for a faster  $\text{NO}_2^-$  removal than in absence of ammonium (Experiment 2C).

Hydroxylamine ( $\text{NH}_2\text{OH}$ ) is an intermediate compound of nitrification previously elucidated as a probable electron donor in bioelectrochemical ammonium oxidation reactors (Vilajeliu-Pons et al., 2018). Experiment 3 evaluated the addition of hydroxylamine at the anode ( $15 \text{ mg N-NH}_2\text{OH L}^{-1}$  in the medium, Table 1). Hydroxylamine spike caused an increase of the current density that peaked at  $90.6 \text{ mA m}^{-2}$  (Fig. 3), which was a value higher than the one observed after the addition of nitrite ( $10.5 \text{ mA m}^{-2}$ ). The concentration of hydroxylamine was measured at 1 and 2 h after the spike, but  $\text{NH}_2\text{OH}$  was only detected (and at a low concentration,  $2.1 \text{ mg N-NH}_2\text{OH L}^{-1}$ ) in the sample taken at the anode of reactor A after 1 h. The hydroxylamine removal rate was estimated as  $1082.7 \text{ g N-NH}_2\text{OH m}^{-3} \text{ d}^{-1}$ . Moreover, the concentration of  $\text{NH}_4^+$ ,  $\text{NO}_2^-$  and  $\text{NO}_3^-$  did not change after the addition of  $\text{NH}_2\text{OH}$  (Fig. 3). The abiotic tests performed with granular graphite (Fig. 4S) showed that, in the absence of bacteria, hydroxylamine was electrochemically oxidized to nitrite and subsequently to nitrate, reinforcing the hypothesis that microbial activity was needed to reduce intermediate oxidized species such as  $\text{NH}_2\text{OH}$ ,  $\text{NO}_3^-$ ,  $\text{NO}_2^-$  or nitric oxide (NO) to  $\text{N}_2$ .

The current density peak observed in the BES tests was assumed to be generated by the anodic oxidation of hydroxylamine, either electrochemically or bioelectrochemically (oxidation of  $\text{NH}_2\text{OH}$  to nitric oxide (NO), a reaction that is catalyzed by hydroxylamine oxidoreductase (HAO), releasing 3 electrons (Caranto and Lancaster, 2017)). Considering the electric current and the  $\text{NH}_2\text{OH}$  removal observed in Experiment 3, the coulombic efficiency for the oxidation of  $\text{NH}_2\text{OH}$  to NO was  $70 \pm 13\%$  (i.e. for a 3-electrons reaction). The nitric oxide generated could be reduced to  $\text{N}_2$  by denitrification instead of ANAMMOX. Although nitric oxide is used as an electron acceptor for  $\text{NH}_4^+$  oxidation

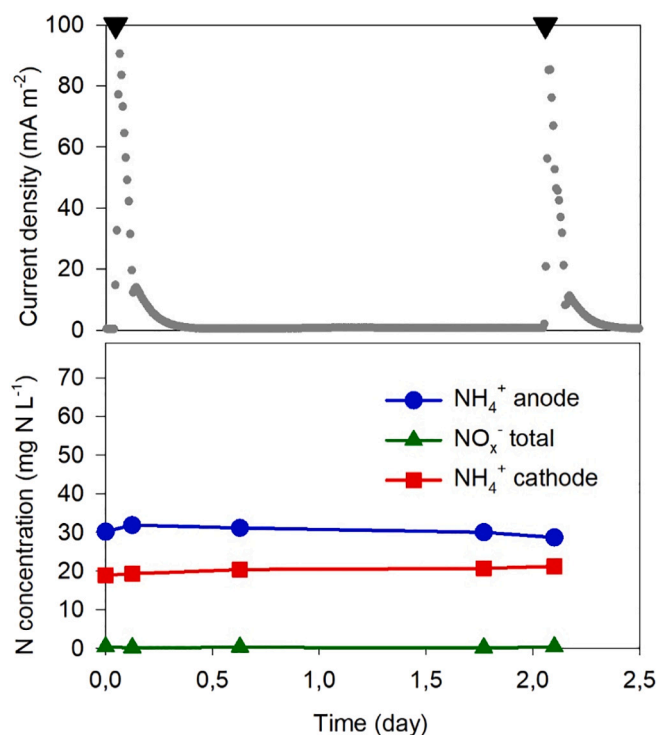


**Fig. 3.** Representative batch test for Experiment 3 in Reactor A. Evolution of nitrogen species concentration ( $\text{NO}_x^-$  represents the total concentration of  $\text{NO}_2^-$  and  $\text{NO}_3^-$  in both chambers) and current density after a pulse of  $\text{NH}_2\text{OH}$  at the anode in Reactor A. Black triangles in the top mark the times when hydroxylamine was added at the anode. Please, note changes in scale for comparison with Figs. 1 and 2.

during ANAMMOX (Hu et al., 2019), no changes in the ammonium concentration were detected during  $\text{NH}_2\text{OH}$  removal in the current study. For similar reasons, electro-ANAMMOX may not have been responsible for the removal of the hydroxylamine added in this Experiment 3, as  $\text{NH}_4^+$  serves as an electron donor for the reduction of  $\text{NH}_2\text{OH}$  to  $\text{N}_2\text{H}_4$  in electro-ANAMMOX (Shaw et al., 2020).

Finally,  $\text{NH}_2\text{OH}$  could also be directly oxidized to  $\text{N}_2$  by a newly discovered hydroxylamine oxidase found in *Alcaligenes* sp. HO-1 (Wu et al., 2021). However, it is still unclear whether *Alcaligenes* sp. HO-1 can use an anode as an electron acceptor for this reaction. Recent experiments with this strain in the author's group pointed out an electrochemical potential of HO-1 strain for some oxidizing steps (unpublished results). Nevertheless, if  $\text{NH}_2\text{OH}$  oxidation to  $\text{N}_2$  reaction was considered (1-electron reaction), the coulombic efficiency for the bioelectrochemical oxidation of  $\text{NH}_2\text{OH}$  would be  $210 \pm 39\%$ , so even though this process could be occurring in the reactor, hydroxylamine should be first oxidized to other more-oxidized nitrogen species (such as  $\text{NO}$  or  $\text{NO}_2^-$ ) to explain the whole of the current density observed.

### 3.3. Performance under a nitrate-rich medium

The removal of nitrate was also studied using different approaches: A) addition of  $\text{NO}_3^-$  to the cathode with  $\text{NH}_4^+$  present at the anode (Experiment 4A Table 1), B) addition of  $\text{NO}_3^-$  to the anode with  $\text{NH}_4^+$  present at the anode (Experiment 4B, Table 1) and, C) addition of  $\text{NO}_3^-$  to the anode with no  $\text{NH}_4^+$  present at the anode (Experiment 4C, Table 1).

In the presence of nitrate, the current density declined ( $0.12 \text{ mA m}^{-2}$  on average) compared to the values observed in presence of ammonium alone ( $0.44 \text{ mA m}^{-2}$ ). When nitrate was fully removed from the system, current density rose again to its previous levels ( $0.47 \text{ mA m}^{-2}$ ) (Fig. 4). It suggested a plug-unplug mechanism, with current being interrupted by

the presence of nitrate and restored after  $\text{NO}_3^-$  had been removed completely. Nitrate removal in Experiments 4A ( $83.0 \text{ g N-NO}_3^- \text{ m}^{-3} \text{ d}^{-1}$  at the cathode), 4B ( $74.6 \text{ g N-NO}_3^- \text{ m}^{-3} \text{ d}^{-1}$  at the anode), and 4C ( $29.5 \text{ g N-NO}_3^- \text{ m}^{-3} \text{ d}^{-1}$  at the anode) (Table 2) occurred at a faster rate than the  $\text{NH}_4^+$  removal observed under ammonium rich-medium ( $4.8 \text{ g N-NH}_4^+ \text{ m}^{-3} \text{ d}^{-1}$  in the anode, Experiment 1 in Section 3.1). According to the estimated rates, it was concluded that ammonium could not have ended up in any detectable nitrate accumulation in the reactor.

Nitrate removal rates were about three times faster in the presence of ammonium ( $83.0$  and  $74.6 \text{ g N-NO}_3^- \text{ m}^{-3} \text{ d}^{-1}$ ) compared to  $29.5 \text{ g N-NO}_3^- \text{ m}^{-3} \text{ d}^{-1}$  in the absence of ammonium. Similar behaviour was observed with nitrite (Section 3.2) suggesting that  $\text{NH}_4^+$  was accelerating the reduction of nitrogen oxides in the system. However, the effect of nitrate over the ammonium removal rate was unclear, as the anodic  $\text{NH}_4^+$  removal was faster in the presence of nitrate at the cathode (Experiment 4B -  $11.9 \text{ g N-NH}_4^+ \text{ m}^{-3} \text{ d}^{-1}$ ) than in the presence of nitrate at the anode (Experiment 4A -  $3.5 \text{ g N-NH}_4^+ \text{ m}^{-3} \text{ d}^{-1}$ ) or in the presence of ammonium alone (Experiment 1 -  $4.8 \text{ g N-NH}_4^+ \text{ m}^{-3} \text{ d}^{-1}$ ). Electricity-driven nitrate removal was discarded since the number of electrons transferred from the anode to the cathode could only account for 2% of the nitrate removal (considering 5 electrons are needed for the reduction of  $\text{NO}_3^-$  to  $\text{N}_2$ ) in all the experiments performed with a nitrate-rich medium (4A, 4B and 4C), (Table 2).

### 3.4. Analysis of the BES microbiome

Samples from bulk and biofilm compartments of both anodes and cathodes were taken from the two duplicate reactors to determine the major microbial players contributing to the above set of reactions. Samples were taken after 450 days of operation (by that time, experiment 2B was being tested, Table 1). On average, 56,510 sequences were obtained per sample (ranging from 33,682 to 78,458). Sequences clustered in a total of 841 amplicon sequence variants (ASV).

At the phylum level, no consistent differences were observed for anode and cathode compartments if the two BES reactors were considered together (Fig. 5). More than half of the ASV (488, accounting for 310,900 total reads) could be resolved at the genus level using a bootstrap level of 80. Archaeal signatures (mainly identified as *Methanobacterium* and *Methanobrevibacter*) were found at low abundances (< 1%) and almost specifically in Reactor A, both in the anode and the cathode compartments. Most sequences belonged to the phylum *Proteobacteria*, *Actinobacteria*, *Bacteroidetes* and *Chloroflexi*. Differences according to the different compartments in the reactors (anode-cathode and bulk-biofilm) occurred at lower taxonomic ranks and revealed interesting differences. For instance, *Achromobacter* spp. were found as the most dominant bacteria in the anodic biofilm of the two reactors (50 to 60%). The relative abundance decreased to 13 and 26% in the cathode of reactors A and B, respectively. A lower relative abundance of *Achromobacter* in the bulk liquid compared to biofilm samples was observed, which suggested an active role of these bacteria in biofilm formation and putative electrode-assisted nitrogen transformations. *Achromobacter* species have been related to heterotrophic simultaneous nitrification and denitrification (Padhi and Maiti, 2017) and heterotrophic nitrification (Ahamed Basha et al., 2018). Heterotrophic nitrification has been more deeply studied with *Alcaligenes* sp. (Wu et al., 2021). According to the latest findings of Wu and co-workers (2021), the heterotrophic nitrifier *Alcaligenes* presents a novel oxidase that can oxidize hydroxylamine directly to  $\text{N}_2$ . Hence, it cannot be discarded a similar role of such a mechanism in *Achromobacter*. Another key enzyme in *Alcaligenes* heterotrophic nitrification, the pyruvic oxime dioxygenase (POD), has significant similarities to *Achromobacter* POD (Tsujino et al., 2017). Moreover, *Achromobacter* could use alternative electron donors, such as  $\text{Mn}^{2+}$ , for denitrification (Su et al., 2018) and it has been found in either anodic biofilm (Ceballos-Escalera et al., 2021) or cathodic biofilms (Zhang et al., 2011) of different BES, suggesting that *Achromobacter* may be able to use electrodes as electron donor/acceptors for nitrification/

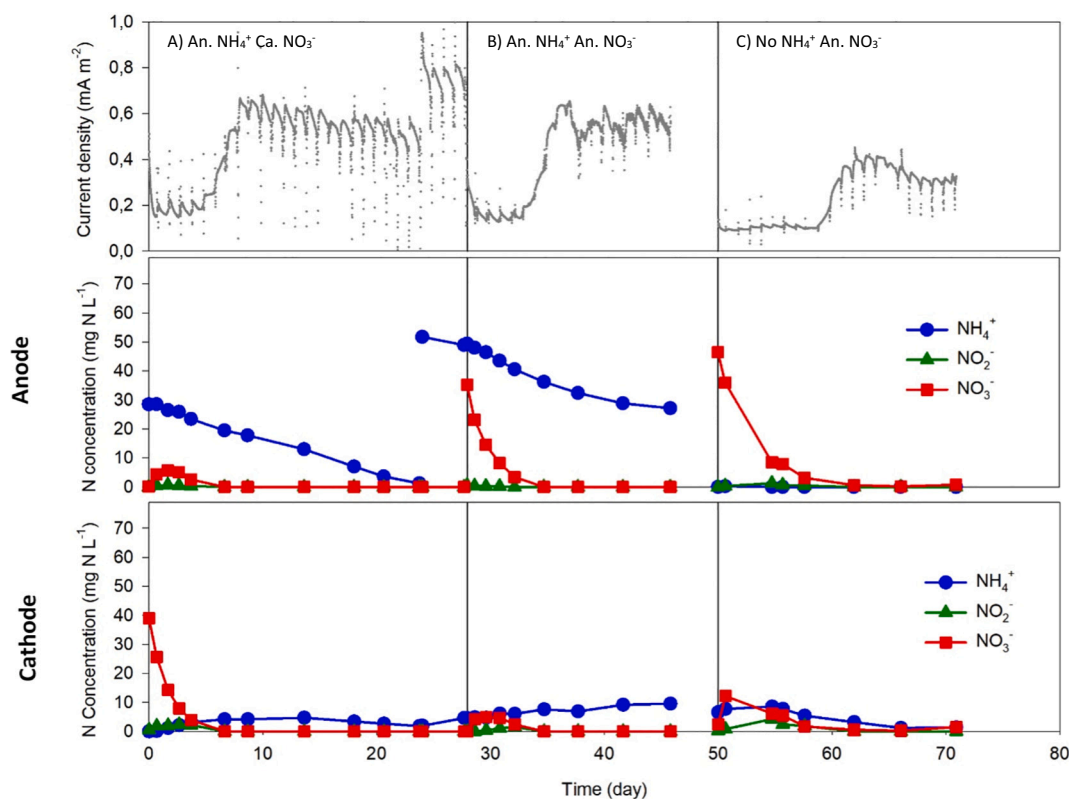


**Fig. 4.** Representatives batches for Experiments 4 in Reactor A. Evolution of nitrogen species concentration and current density (top), nitrogen species concentration at the anode (middle) and nitrogen species at the cathode (bottom). A) Experiment 4A: addition of  $\text{NO}_3^-$  to the cathode with  $\text{NH}_4^+$  present at the anode (left). B) Experiment 4B: addition of  $\text{NO}_3^-$  to the anode with  $\text{NH}_4^+$  present at the anode (centre). C) Experiment 4C: addition of  $\text{NO}_3^-$  to the anode with no  $\text{NH}_4^+$  present at the anode (right).

denitrification processes.

*Denitratisoma*, an autotrophic denitrifier (Deng et al., 2016), tended to accumulate in the cathode compartment of both reactors ( $10.0 \pm 5.2\%$ ) compared to the anode ( $4.1 \pm 2.4\%$ ). *Denitratisoma* sp. has previously been described as being dominant in the cathodic biofilm of a denitrifying BES (Ma et al., 2015), so it might have contributed to the removal of nitrogen reduced species in our system. *Nitrosomonas* sp. and *Nitrospira* sp. were the only nitrifying bacteria that could be detected. In both cases, they showed a preference for growing on the biofilm. Relative abundance of *Nitrosomonas* was around 1% of sequence reads in the anodic biofilm and it decreased to almost undetectable values in the bulk liquid of the two reactors. The maximum relative concentration (6.3%) was found in the cathodic biofilm of reactor A but not in reactor B ( $<0.3\%$ ). A similar distribution was detected for *Nitrospira* albeit much lower relative abundances were recovered (below 0.25%).

Providing the kinetics observed in the two reactors were similar and the differences in the relative abundance of ANAMMOX bacteria, we hypothesized ANAMMOX was a secondary reaction in the reactors that could also have a role in the simultaneous reduction of nitrite in the presence of ammonium. “*Candidatus Kuenenia*” (*Brocadiales*) and “*Candidatus Anammoximicrobium*” (tentatively classified within *Pir-ellulales*) were the only predicted ANAMMOX bacteria (Kartal et al., 2013) found in the studied samples (Fig. S6). “*Candidatus Kuenenia*” was more abundant, showing the highest relative abundances in the anodic biofilm of both reactors (1 to 2% of sequences). Relative densities decreased below 0.3% in the bulk samples and the cathode biofilm, suggesting a selective enrichment on the electrode surface.

### 3.5. Perspectives for anoxic ammonium removal using BES and the elucidation of the pathways for ammonium removal in BES

Recent advances on ANAMMOX and nitrifying bacteria behaviour on polarized anodes (Shaw et al., 2020; Vilajeliu-Pons et al., 2018) has allowed the scientific community to light up a near future where the key components of wastewater (organic matter and nitrogen) can be fully removed with renewable electricity supply and without the need of external electron donors and acceptors. This opens the door to the implementation of BES-based technologies for removing different kinds of wastewaters involving organic matter and nitrogen at low C/N ratios. For large-scale applications, such as the current operating wastewater treatment plants, the competence and lower operational cost of BES-based technologies might not be enough to replace them because the high capital outlays that has been invested in still needs to be paid off. However, in the current transition from centralization to decentralization (Rabaey et al., 2020), BES-based technologies might be a reasonable alternative to current wastewater treatment technologies. In addition, the development of technologies able to carry out complex processes, such as electricity-driven ammonium removal, with mixed cultures that do not require special care is a tool to implement sanitation solutions. For this reason, the work presented here can contribute to the implementation of BES-based sanitation solutions by providing a better understanding of the underlying processes behind anoxic ammonium removal in BES colonized by nitrifying bacteria.

Autotrophic ammonium removal in BES without accumulation of intermediary metabolites can be viewed as a complex process (Fig. 6). Experiments performed with the sole presence of ammonium (Experiment 1) resulted in current densities corresponding to the use of 3 electrons per molecule of  $\text{NH}_4^+$  oxidation to  $\text{N}_2$  (theoretical value). Different nitrogen dynamics were revealed inside the reactor, which

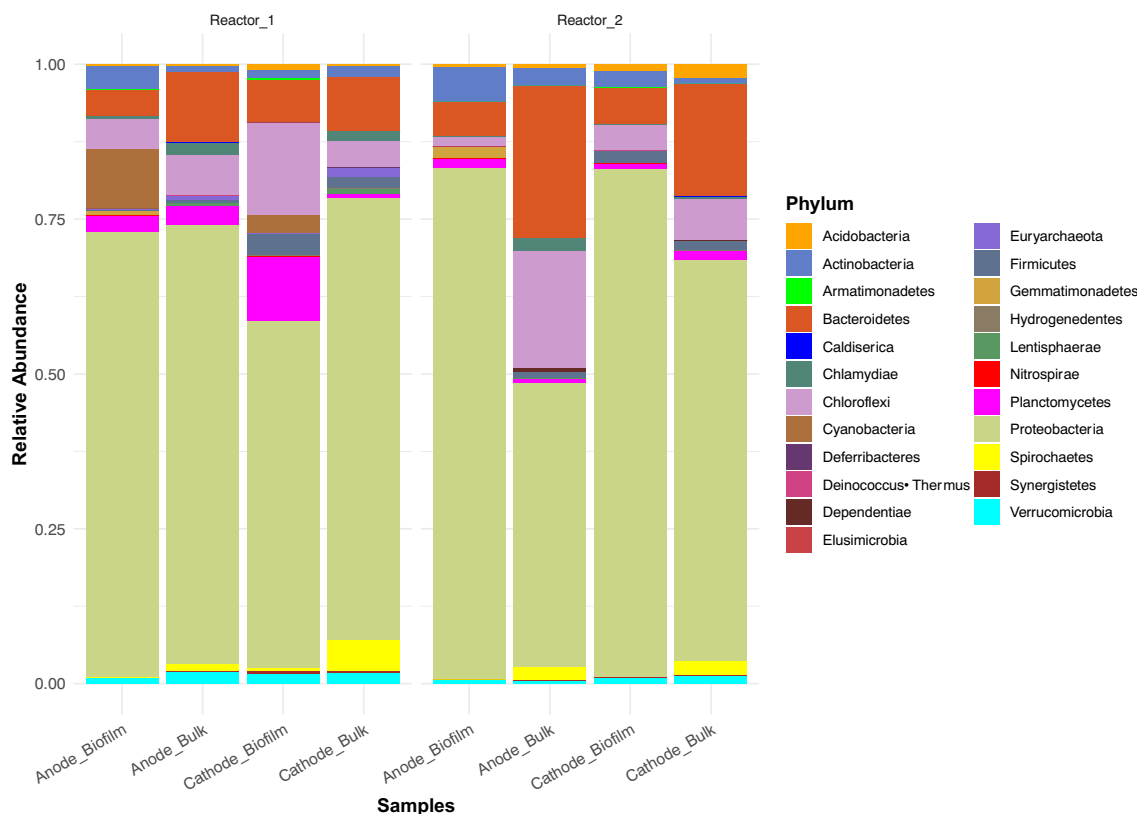


Fig. 5. Relative abundance (number of sequences) of main Phyla in the studied reactors. Samples are organized as per reactor and compartments (Anode-Cathode, bulk-biofilm) inside the reactor.

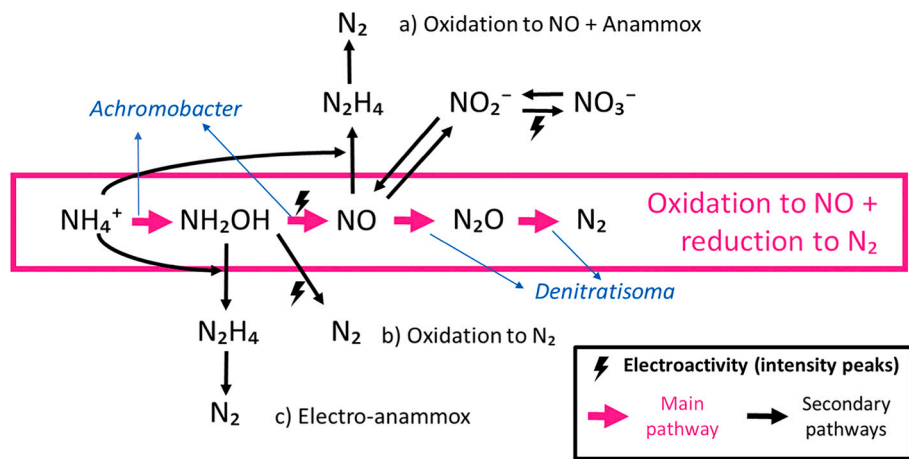


Fig. 6. Summary of the reactions involving nitrogen compounds that could be occurring in the BES during this study. The main ammonium removal pathway proposed is the bioelectrochemical oxidation of  $\text{NH}_4^+$  to NO, possibly performed by *Achromobacter*, followed by the reduction of NO to  $\text{N}_2$ , which could be carried out by *Denitratisoma* (all this route is highlighted in pink), while other 3 secondary routes are also considered: a) bioelectrochemical oxidation of  $\text{NH}_4^+$  to NO followed by anammox, b) bioelectrochemical oxidation of  $\text{NH}_4^+$  to  $\text{N}_2$  and c) electro-anammox. The reactions of  $\text{NH}_2\text{OH}$  oxidation and  $\text{NO}_2^-$  oxidation are distinguished with an exclamation mark because they are the processes showing the most intense electrochemical response in this study. (For interpretation of the references to colour in this figure legend, the reader is referred to the web version of this article.)

suggested the occurrence of different ammonium removal pathways. The preeminent one could be a first oxidation of ammonium to hydroxylamine, followed by a second oxidation of this later. Hydroxylamine oxidation was found to be a highly electroactive reaction, in accordance with previous studies (Vilajeliu-Pons et al., 2018). Taking all results together, the final product of hydroxylamine oxidation was not clear, although an implication of the recently described hydroxylamine oxidase converting  $\text{NH}_2\text{OH}$  to  $\text{N}_2$  has been speculated (Wu et al., 2021). This possibility was reinforced due to the large presence of *Achromobacter* spp. in the reactors, a microorganism with significant similarities to *Alcaligenes*. The electric current generated during  $\text{NH}_2\text{OH}$  removal indicates that an alternative, more-oxidized, compound must be the major product of hydroxylamine oxidation, probably nitric oxide (NO),

which can be rapidly converted into nitrite (oxidation) or nitrous oxide (reduction) due to its instability. Although the most reasonable outcome for nitric oxide in an oxidative environment like the anode would be the production of nitrite, no accumulation of it was detected in the reactor after the addition of  $\text{NH}_2\text{OH}$  (Experiment 3), suggesting that nitric oxide oxidation may be a minor pathway. Moreover, no  $\text{N}_2\text{O}$  was detected in any of the experiments, and a complete reduction of NO to  $\text{N}_2$  was considered.

Data from experiments where nitrate was added (Experiment 4) were analysed to elucidate the possible electron donors used for NO reduction. Results showed that different electron donor sources could be used for nitrate reduction. The cathodic electrode could be responsible for only a small part of the  $\text{NO}_3^-$  reduction, as the current could only



explain 2% of  $\text{NO}_3^-$  conversion into  $\text{N}_2$  observed in experiments 4A, 4B and 4C. Heterotrophic denitrification had a minor role in this system because no organic matter was added. Thus, there was a deficiency of electrons to explain the whole nitrate reduction observed, which suggested the presence of other mechanisms. For example, an additional hypothesis could be linked to direct interspecies electron transfer (DIET) by coupling oxidation of reduced nitrogen species, such as ammonium, with nitrate reduction. This hypothesis could be supported by the observation of current density suppression when nitrate was spiked to the system in presence of ammonium (Experiment 4A and 4B). However, DIET cannot explain the whole of the results observed, since nitrate was also removed in absence of ammonium or any other feasible electron donor (Experiment 4C).

Nitrite tests (Experiments 2) revealed that  $\text{NO}_2^-$  was electrochemically and bioelectrochemically oxidized to  $\text{NO}_3^-$  since nitrite removal could be linked to a significant spike in current density with and without ammonium presence in the reactor. A transient accumulation of nitrate in the system was observed, with a final complete conversion into  $\text{N}_2$ .

Finally, the presence of  $\text{N}_2\text{H}_4$  was detected both in the cathodic and anodic chamber when both nitrite and ammonium were present in the system (Experiments 2A and 2B), while microbial analyses revealed the presence ANAMMOX bacteria in the bulk a liquid and, particularly, on the anode surface (“*Candidatus Kuenenia*” and “*Candidatus Anammoximicrobium*”). It suggested that ANAMMOX reactions could also be having a role in the system. In this case, nitrite, nitric oxide, or the electrode may serve as electron acceptors for the oxidation of ammonium to nitrogen gas. However, ANAMMOX bacteria were found at a lower abundance than nitrifiers and denitrifiers. ANAMMOX and electro-ANAMMOX could potentially be involved in  $\text{NO}$  and  $\text{NH}_2\text{OH}$  removal, respectively. However, no  $\text{NH}_4^+$  consumption was observed during  $\text{NH}_2\text{OH}$  (and subsequently,  $\text{NO}$ ) removal, indicating that this could only be minority pathways (Fig. 6).

Taking it all together, the system studied here presented a complex microbial community that was able to carry out a plethora of nitrogen removal mechanisms. From a black-box perspective, the system was able to handle different nitrogen compounds that are usually present in wastewater (i.e. ammonium, nitrite and nitrate) and convert them into dinitrogen gas without the presence of organic matter. The gained know-how will be used to improve the reactor design and operation leading to an increase in the current ammonium removal rates to compete with ANAMMOX or other bioelectrochemically-induced ammonium oxidation.

#### 4. Conclusions

Ammonium was converted into dinitrogen gas in an anoxic BES. A coulombic efficiency of 108% was observed, suggesting that the anodic electrode acted as the electron acceptor for this process. Two highly electroactive reactions were identified (hydroxylamine and nitrite oxidation). Data obtained from nitrite and nitrate tests suggested that both denitrification and ANAMMOX based reactions could take place in the BES to close the conversion of  $\text{NH}_4^+$  into  $\text{N}_2$ . In fact, the dominant bacteria in the BES was a nitrifier (*Achromobacter* spp.), but the microbial community in the reactor included also ANAMMOX species (*Candidatus Kuenenia* and *Candidatus Anammoximicrobium*) and denitrifying bacteria (*Denitratisoma* sp.).

#### CRediT authorship contribution statement

**Miguel Osset-Álvarez:** Conceptualization, Data curation, Investigation, Methodology, Writing – original draft. **Narcis Pous:** Conceptualization, Data curation, Investigation, Methodology, Writing – review & editing. **Paola Chiluiza-Ramos:** Data curation, Investigation, Writing – review & editing. **Lluís Bañeras:** Conceptualization, Funding acquisition, Methodology, Supervision, Investigation, Writing – review & editing. **M. Dolores Balaguer:** Conceptualization, Funding acquisition,

Methodology, Supervision, Writing – review & editing. **Sebastià Puig:** Conceptualization, Funding acquisition, Methodology, Supervision, Project administration, Writing – review & editing.

#### Declaration of competing interest

The authors declare that they have no known competing financial interests or personal relationships that could have appeared to influence the work reported in this paper.

#### Acknowledgements

This work was funded through the European Union's Horizon 2020 project ELECTRA [no. 826244]. M. O-A. was supported by a grant from University of Girona (IFUdG2018/50). S.P. is a Serra Húnter Fellow (UdG-AG-575) and acknowledges the funding from the ICREA Academia award. LEQUiA [2017-SGR-1552] and Ecoaqua [2017SGR- 548] have been recognized as consolidated research groups by the Catalan Government.

#### Appendix A. Supplementary data

Supplementary data to this article can be found online at <https://doi.org/10.1016/j.biteb.2022.100975>.

#### References

- Ahamed Basha, K., Joseph, T.C., Lalitha, K.V., Vineetha, D., Rathore, G., Tripathi, G., Prasad, K.P., 2018. Nitrification potential of *Achromobacter xylosoxidans* Isolated from Fresh Water Finfish Farms of Kerala, India. *Int. J. Curr. Microbiol. App. Sci.* 7, 2645–2654. <https://doi.org/10.20546/ijcmas.2018.708.273>.
- Callahan, B.J., McMurdie, P.J., Rosen, M.J., Han, A.W., Johnson, A.J.A., Holmes, S.P., 2016. DADA2: High-resolution sample inference from Illumina amplicon data. *Nat. Methods* 13, 581–583. <https://doi.org/10.1038/nmeth.3869>.
- Caranto, J.D., Lancaster, K.M., 2017. Nitric oxide is an obligate bacterial nitrification intermediate produced by hydroxylamine oxidoreductase. *PNAS* 114. <https://doi.org/10.1073/pnas.1704504114>.
- Ceballos-Escalera, A., Pous, N., Chiluiza-Ramos, P., Korth, B., Harnisch, F., Bañeras, L., Balaguer, M.D., Puig, S., 2021. Electro-bioremediation of nitrate and arsenite polluted groundwater. *Water Res.* 190, 116748 <https://doi.org/10.1016/j.watres.2020.116748>.
- Deng, S., Li, D., Yang, X., Xing, W., Li, J., Zhang, Q., 2016. Biological denitrification process based on the Fe(0)-carbon micro-electrolysis for simultaneous ammonia and nitrate removal from low organic carbon water under a microaerobic condition. *Bioresour. Technol.* 219, 677–686. <https://doi.org/10.1016/j.biortech.2016.08.014>.
- Gabarró, J., Ganigué, R., Gich, F., Rusalleda, M., Colprim, J., 2012. Effect of temperature on AOB activity of a partial nitrification SBR treating landfill leachate with extremely high nitrogen concentration. *Bioresour. Technol.* 126, 283–289. <https://doi.org/10.1016/j.biortech.2012.09.011>.
- Hu, Z., Wessels, H.J.C.T., Van Alen, T., Jetten, M.S.M., Kartal, B., 2019. Nitric oxide-dependent anaerobic ammonium oxidation. *Nat. Commun.* 10, 1–7. <https://doi.org/10.1038/s41467-019-09268-w>.
- Kartal, B., Maalcke, W.J., De Almeida, N.M., Cirpus, I., Gloerich, J., Geerts, W., Op Den Camp, H.J.M., Harhangi, H.R., Janssen-Megens, E.M., Francoijs, K.-J., Stunnenberg, H.G., Keltjens, J.T., Jetten, M.S.M., Strous, M., 2011. Molecular mechanism of anaerobic ammonium oxidation. *Nature* 479, 127–130. <https://doi.org/10.1038/nature10453>.
- Kartal, B., de Almeida, N.M., Maalcke, W.J., Op den Camp, H.J.M., Jetten, M.S.M., Keltjens, J.T., 2013. How to make a living from anaerobic ammonium oxidation. *FEMS Microbiol. Rev.* 37, 428–461. <https://doi.org/10.1111/1574-6976.12014>.
- Kim, J.R., Zuo, Y., Regan, J.M., Logan, J.M., 2008. Analysis of ammonia loss mechanisms in microbial fuel cells treating animal wastewater. *Biotechnol. Bioeng.* 99, 1120–1127. <https://doi.org/10.1002/bit.21687>.
- Koffi, N.J., Okabe, S., 2021. Bioelectrochemical anoxic ammonium nitrogen removal by an MFC driven single chamber microbial electrolysis cell. *Chemosphere* 274, 129715. <https://doi.org/10.1016/j.chemosphere.2021.129715>.
- Kozich, J., Westcott, S.L., Baxter, N.T., Highlander, S.K., Schloss, P.D., 2013. Development of a dual-index sequencing strategy and curation pipeline for analyzing amplicon sequence data on the miseq illumina sequencing platform. *Appl. Environ. Microbiol.* 79, 5112–5120. <https://doi.org/10.1128/AEM.01043-13>.
- Lai, A., Aulenta, F., Mingazzini, M., Palumbo, M.T., Papini, M.P., Verdini, R., Majone, M., 2017. Bioelectrochemical approach for reductive and oxidative dechlorination of chlorinated aliphatic hydrocarbons (CAHs). *Chemosphere* 169, 351–360. <https://doi.org/10.1016/j.chemosphere.2016.11.072>.
- Ma, J., Wang, Z., He, D., Li, Y., Wu, Z., 2015. Long-term investigation of a novel electrochemical membrane bioreactor for low-strength municipal wastewater treatment. *Water Res.* 78, 98–110. <https://doi.org/10.1016/j.watres.2015.03.033>.

- McMurdie, P.J., Holmes, S., 2012. Phyloseq: a bioconductor package for handling and analysis of high-throughput phylogenetic sequence data. In: *Biocomputing 2012*. World Scientific, pp. 235–246.
- Oshiki, M., Ali, M., Shinyako-Hata, K., Satoh, H., Okabe, S., 2016. Hydroxylamine-dependent anaerobic ammonium oxidation (anammox) by “*Candidatus Brocadia sinica*”. *Environ. Microbiol.* 18, 3133–3143. <https://doi.org/10.1111/1462-2920.13355>.
- Padhi, S.K., Maiti, N.K., 2017. Molecular insight into the dynamic central metabolic pathways of *Achromobacter xylooxidans* CF-S36 during heterotrophic nitrogen removal processes. *J. Biosci. Bioeng.* 123, 46–55. <https://doi.org/10.1016/j.jbiosc.2016.07.012>.
- Qu, B., Fan, B., Zhu, S., Zheng, Y., 2014. Anaerobic ammonium oxidation with an anode as the electron acceptor. *Environ. Microbiol. Rep.* 6, 100–105. <https://doi.org/10.1111/1758-2229.12113>.
- Rabaey, K., Ossieur, W., Verhaege, M., Verstraete, W., 2005. Continuous microbial fuel cells convert carbohydrates to electricity. *Water Sci. Technol.* 52, 515–523.
- Rabaey, K., Vandekerckhove, T., de Walle, A.V., Sedlak, D.L., 2020. The third route: using extreme decentralization to create resilient urban water systems. *Water Res.* 185 <https://doi.org/10.1016/j.watres.2020.116276>.
- Ruiz-Urigüen, M., Steingart, D., Jaffé, P.R., 2019. Oxidation of ammonium by *Feammox* Acidimicrobiaceae sp. A6 in anaerobic microbial electrolysis cells. *Environ. Sci. Water Res. Technol.* 5, 1582–1592. <https://doi.org/10.1039/c9ew00366e>.
- Shaw, D.R., Ali, M., Katuri, K.P., Gralnick, J.A., Reimann, J., Mesman, R., Van Niftrik, L., Jetten, M.S.M., Saikaly, P.E., 2020. Extracellular electron transfer-dependent anaerobic oxidation of ammonium by anammox bacteria. *Nat. Commun.* 11 <https://doi.org/10.1038/s41467-020-16016-y>.
- Siegert, M., Tan, A., 2019. Electric stimulation of ammonotrophic methanogenesis. *Front. Energy Res.* 7, 1–5. <https://doi.org/10.3389/fenrg.2019.00017>.
- Su, J., Liang, D., Lian, T., 2018. Comparison of denitrification performance by bacterium *Achromobacter* sp. A14 under different electron donor conditions. *Chem. Eng. J.* 333, 320–326. <https://doi.org/10.1016/j.cej.2017.09.129>.
- Tsujino, S., Uematsu, C., Dohra, H., Fujiwara, T., 2017. In: *Pyruvic Oxime Dioxygenase From Heterotrophic Nitrifier Alcaligenes faecalis Is a Nonheme Fe (II)-dependent Enzyme Homologous to Class II Aldolase*, 7, pp. 1–8. <https://doi.org/10.1038/srep39991>.
- Tutar Oksuz, S., Beyenal, H., 2021. Enhanced bioelectrochemical nitrogen removal in flow through electrodes. *Sustain. Energy Technol. Assess.* 47, 101507 <https://doi.org/10.1016/j.seta.2021.101507>.
- Van Teeseling, M.C.F., Neumann, S., Van Niftrik, L., 2013. The anammoxosome organelle is crucial for the energy metabolism of anaerobic ammonium oxidizing bacteria. *J. Mol. Microbiol. Biotechnol.* 23, 104–117. <https://doi.org/10.1159/000346547>.
- Vilajeliu-Pons, A., Bañeras, L., Puig, S., Molognoni, D., Vilà-Rovira, A., Amo, E.H., Del Balaguer, M.D., Colprim, J., 2016. External resistances applied to MFC affect core microbiome and swine manure treatment efficiencies. *PLoS One* 11, 1–19. <https://doi.org/10.1371/journal.pone.0164044>.
- Vilajeliu-Pons, A., Koch, C., Balaguer, M.D., Colprim, J., Harnisch, F., Puig, S., 2018. Microbial electricity driven anoxic ammonium removal. *Water Res.* 130, 168–175. <https://doi.org/10.1016/j.watres.2017.11.059>.
- Wu, M., Hou, T., Liu, Y., Miao, L., Ai, G., Ma, L., Zhu, H., Zhu, Y., Gao, X., Herbold, C.W., 2021. Novel *Alcaligenes ammonioxydans* sp. nov. from wastewater treatment sludge oxidizes ammonia to N<sub>2</sub> with a previously unknown pathway. *Environ. Microbiol.* 23, 6965–6980. <https://doi.org/10.1111/1462-2920.15751>.
- Zhan, G., Zhang, L., Tao, Y., Wang, Y., Zhu, X., Li, D., 2014. Anodic ammonia oxidation to nitrogen gas catalyzed by mixed biofilms in bioelectrochemical systems. *Electrochim. Acta* 135, 345–350. <https://doi.org/10.1016/j.electacta.2014.05.037>.
- Zhang, G.D., Zhao, Q.L., Jiao, Y., Zhang, J.N., Jiang, J.Q., Ren, N., Kim, H., 2011. Improved performance of microbial fuel cell using combination biocathode of graphite fiber brush and graphite granules. *J. Power Sources* 196, 6036–6041. <https://doi.org/10.1016/j.jpowsour.2011.03.096>.
- Zhou, Q., Yang, N., Zheng, D., Zhang, L., Tian, C., Yang, Q., Li, D., 2021. Electrode-dependent ammonium oxidation with different low C/N ratios in single-chambered microbial electrolysis cells. *Bioelectrochemistry* 142. <https://doi.org/10.1016/j.bioelechem.2021.107889>.
- Zhu, T., Zhang, Y., Bu, G., Quan, X., Liu, Y., 2016. Producing nitrite from anodic ammonia oxidation to accelerate anammox in a bioelectrochemical system with a given anode potential. *Chem. Eng. J.* 291, 184–191. <https://doi.org/10.1016/J.CEJ.2016.01.099>.
- Zhu, Ting, T., Zhang, Bin, Y., Liu, Wen, Y., Zhao, Sheng, Z., 2021. Electrostimulation enhanced ammonium removal during Fe(III) reduction coupled with anaerobic ammonium oxidation (Feammox) process. *Sci. Total Environ.* 751, 141703 <https://doi.org/10.1016/j.scitotenv.2020.141703>.